

Rare Z -decay into light CP-odd Higgs bosons: a comparative study in different new physics models

Junjie Cao¹, Zhaoxia Heng², Jin Min Yang²

¹ *Department of Physics, Henan Normal University, Xinxiang 453007, China*

² *Key Laboratory of Frontiers in Theoretical Physics,
Institute of Theoretical Physics, Academia Sinica, Beijing 100190, China*

Abstract

Various new physics models predict a light CP-odd Higgs boson (labeled as a) and open up new decay modes for Z -boson, such as $Z \rightarrow \bar{f}fa$, $Z \rightarrow aaa$ and $Z \rightarrow a\gamma$, which could be explored at the GigaZ option of the ILC. In this work we evaluate these rare decays in several new physics models, namely the Type-II 2HDM, the lepton-specific 2HDM, the nMSSM and the NMSSM. We find that in the parameter space allowed by current experiments, the branching ratios can reach 10^{-4} for $Z \rightarrow \bar{f}fa$ ($f = b, \tau$), 10^{-3} for $Z \rightarrow aaa$ and 10^{-8} for $Z \rightarrow a\gamma$, which should be accessible at the GigaZ option. Moreover, since different models predict different patterns of the branching ratios, the measurement of these rare decays at the GigaZ may be utilized to distinguish the models.

PACS numbers: 13.38.Dg,12.60.Fr,14.80.Da

I. INTRODUCTION

The LEP experiments at the resonance of Z -boson have tested the Standard Model (SM) at quantum level, measuring the Z -decay to fermion pairs with an accuracy of one part in ten thousands. The good agreement of the LEP data with the SM predictions have severely constrained the behavior of new physics at the Z -pole. Taking these achievements into account and also noting the expected sensitivity to Z -decays is 10^{-8} at the GigaZ option of the ILC [1] (compared with 10^{-5} at LEP), one can imagine that the physics of Z -boson will again play the central role in the frontier of particle physics if the GigaZ comes true in the future. In light of this, the Z -boson properties, especially its exotic or rare decays which are widely believed to be sensitive to new physics, should be investigated comprehensively to evaluate their potential in probing new physics.

Among the rare Z -decays, the flavor changing processes were most extensively studied to explore the flavor texture in new physics [2], and it was found that, although these processes are forbidden or severely suppressed in the SM, their branching ratios in new physics models can be greatly enhanced to 10^{-8} for lepton flavor violation decays [3] and 10^{-6} for quark flavor violation decays [4]. In addition, the Z -decays into light Higgs bosons may also be open in some new physics models and as shown in [5, 6], these exotic decays (not exist in the SM) are quite sensitive to the properties of the Higgs sector in the underlying physics. In this work, we extend the study of [5, 6] by considering more exotic decay channels of Z -boson and perform a comparative study in different new physics models. Our interest to these decays is motivated by some recent studies on the singlet extension of the minimal supersymmetric standard model (MSSM), such as the next-to-minimal supersymmetric standard model (NMSSM) [7, 8] and the nearly minimal supersymmetric standard model (nMSSM) [9], where a light CP-odd Higgs boson a with singlet-dominant component may naturally arise from the spontaneous breaking of some approximate global symmetry like $U_R(1)$ or Peccei-Quinn symmetry [10–12]. These non-minimal supersymmetric models can not only avoid the μ -problem, but also alleviate the little hierarchy by having such a light Higgs boson a [13]. Moreover, we note that even in some simple extensions of the SM like the general two Higgs doublet model (2HDM), a light CP-odd Higgs boson a can not be ruled out by current experiments [6]; instead, a light CP-odd Higgs boson a may help to alleviate the long-standing discrepancy between the SM prediction of the muon anomalous

magnetic moment and its measured value.

So far there is no model-independent lower bound on the Higgs boson mass. In the SM, it must be heavier than 114 GeV, obtained from the null observation of the Higgs boson at LEP experiments. However, due to the more complex structure of the Higgs sector in the extensions of the SM, this lower bound can be significantly relaxed, e.g., for the CP-odd Higgs boson a we have $m_a \gtrsim 1$ GeV in the nMSSM [14], $m_a \gtrsim 0.21$ GeV in the NMSSM [11], $m_a \gtrsim 0.2$ GeV in the 2HDM [6], and $m_a \gtrsim 7$ GeV in the lepton-specific 2HDM (L2HDM) [15]. With such a light CP-odd Higgs boson, the rare Z -decays $Z \rightarrow \bar{f}fa$ ($f = b, \tau$), $Z \rightarrow aaa$ and $Z \rightarrow a\gamma$ are kinematically allowed and thus open a window to new physics (note that $Z \rightarrow aa$ is forbidden due to Bose symmetry). Since these decays have not been studied in a comparative way, we in this work study them comparatively for four models, namely the Type-II 2HDM, the L2HDM [16, 17], the nMSSM and the NMSSM.

This work is organized as follows. In Sec. II we briefly describe the four new physics models. In Sec. III we present the calculations of the rare Z -decays. In Sec. IV we show the numerical results for the branching ratios of the rare Z -decays in various models. Finally, the conclusion is given in Sec. V.

II. THE NEW PHYSICS MODELS

As the most economical way, the SM utilizes one Higgs doublet to break the electroweak symmetry. As a result, the SM predicts only one physics Higgs boson with its properties totally determined by two free parameters. In new physics models, the Higgs sector is usually extended by adding Higgs doublets and/or singlets, and consequently, more physical Higgs bosons are predicted along with more free parameters involved.

The general 2HDM contains two $SU(2)_L$ doublet Higgs fields ϕ_1 and ϕ_2 , and with the assumption of CP-conserving, its scalar potential can be parameterized as[18]:

$$\begin{aligned}
 V = & m_1^2 \phi_1^\dagger \phi_1 + m_2^2 \phi_2^\dagger \phi_2 - (m_3^2 \phi_1^\dagger \phi_2 + H.c.) + \frac{\lambda_1}{2} (\phi_1^\dagger \phi_1)^2 + \frac{\lambda_2}{2} (\phi_2^\dagger \phi_2)^2 \\
 & + \lambda_3 (\phi_1^\dagger \phi_1) (\phi_2^\dagger \phi_2) + \lambda_4 (\phi_1^\dagger \phi_2) (\phi_2^\dagger \phi_1) + \frac{\lambda_5}{2} [(\phi_1^\dagger \phi_2)^2 + H.c.], \quad (1)
 \end{aligned}$$

where λ_i ($i = 1, \dots, 5$) are free dimensionless parameters, and m_i ($i = 1, 2, 3$) are the parameters with mass dimension. After the electroweak symmetry breaking, the spectrum of this Higgs sector includes three massless Goldstone modes, which become the longitudinal

modes of W^\pm and Z bosons, and five massive physical states: two CP-even Higgs bosons h_1 and h_2 , one neutral CP-odd Higgs particle a and a pair of charged Higgs bosons H^\pm . Noting the constraint $v_1^2 + v_2^2 = (246 \text{ GeV})^2$ with v_1 and v_2 denoting the vacuum expectation values (vev) of ϕ_1 and ϕ_2 respectively, we choose

$$m_{h_1}, \quad m_{h_2}, \quad m_a, \quad m_{H^\pm}, \quad \tan \beta, \quad \sin \alpha, \quad \lambda_5 \quad (2)$$

as the input parameters with $\tan \beta = v_2/v_1$, and α being the mixing angle that diagonalizes the mass matrix of the CP-even Higgs fields.

The difference between the Type-II 2HDM and the L2HDM comes from the Yukawa coupling of the Higgs bosons to quark/lepton. In the Type-II 2HDM, one Higgs doublet ϕ_2 generates the masses of up-type quarks and the other doublet ϕ_1 generates the masses of down-type quarks and charged leptons; while in the L2HDM one Higgs doublet ϕ_1 couples only to leptons and the other doublet ϕ_2 couples only to quarks. So the Yukawa interactions of a to fermions in these two models are given by [6, 15]

$$\mathcal{L}_{\text{Yukawa}}^{\text{Type-II}} = \frac{igm_{u_i}}{2m_W} \cot \beta \bar{u}_i \gamma^5 u_i a + \frac{igm_{d_i}}{2m_W} \tan \beta \bar{d}_i \gamma^5 d_i a + \frac{igm_{e_i}}{2m_W} \tan \beta \bar{e}_i \gamma^5 e_i a, \quad (3)$$

$$\mathcal{L}_{\text{Yukawa}}^{\text{L2HDM}} = \frac{igm_{u_i}}{2m_W} \cot \beta \bar{u}_i \gamma^5 u_i a - \frac{igm_{d_i}}{2m_W} \cot \beta \bar{d}_i \gamma^5 d_i a + \frac{igm_{e_i}}{2m_W} \tan \beta \bar{e}_i \gamma^5 e_i a, \quad (4)$$

with i denoting generation index. Obviously, in the Type-II 2HDM the $\bar{b}ba$ coupling and the $\bar{\tau}\tau a$ coupling can be simultaneously enhanced by $\tan \beta$, while in the L2HDM only the $\bar{\tau}\tau a$ coupling is enhanced by $\tan \beta$.

The structure of the nMSSM and NMSSM can be well understood from their superpotentials and corresponding soft-breaking terms, which are given by [19]

$$W_{\text{nMSSM}} = W_{\text{MSSM}} + \lambda \hat{H}_u \cdot \hat{H}_d \hat{S} + \xi_F M_n^2 \hat{S}, \quad (5)$$

$$W_{\text{NMSSM}} = W_{\text{MSSM}} + \lambda \hat{H}_u \cdot \hat{H}_d \hat{S} + \frac{1}{3} \kappa \hat{S}^3, \quad (6)$$

$$V_{\text{soft}}^{\text{nMSSM}} = \tilde{m}_u^2 |H_u|^2 + \tilde{m}_d^2 |H_d|^2 + \tilde{m}_S^2 |S|^2 + (A_\lambda \lambda S H_u \cdot H_d + \xi_S M_n^3 S + h.c.), \quad (7)$$

$$V_{\text{soft}}^{\text{NMSSM}} = \tilde{m}_u^2 |H_u|^2 + \tilde{m}_d^2 |H_d|^2 + \tilde{m}_S^2 |S|^2 + (A_\lambda \lambda S H_u \cdot H_d + \frac{A_\kappa}{3} \kappa S^3 + h.c.), \quad (8)$$

where W_{MSSM} is the superpotential of the MSSM without the μ term, $\hat{H}_{u,d}$ and \hat{S} are Higgs doublet and singlet superfields with $H_{u,d}$ and S being their scalar component respectively, $\tilde{m}_u, \tilde{m}_d, \tilde{m}_S, A_\lambda, A_\kappa$ and $\xi_S M_n^3$ are soft breaking parameters, and λ and κ are coefficients of the Higgs self interactions. Since in the nMSSM, the tadpole terms $\xi_F M_n^2 \hat{S}$ and its soft

breaking term $\xi_S M_n^3 S$ do not induce any interactions, except for the tree-level Higgs boson masses and the minimization conditions, the nMSSM is actually same as the NMSSM with the trilinear singlet term set to zero[14]. Another common feature of the two models is that there is no explicit μ -term in the nMSSM and NMSSM. The effective μ parameter (μ_{eff}) is generated when the scalar component of \hat{S} develops a vev. Just like the 2HDM where we use the vevs of the Higgs fields as fundamental parameters, we choose $\lambda, \kappa, \tan \beta, \mu_{\text{eff}} = \lambda \langle S \rangle, A_\kappa$ and $m_A^2 = \frac{2\mu}{\sin 2\beta} (A_\lambda + \frac{\kappa\mu}{\lambda})$ as input parameters for the NMSSM[19] and $\lambda, \tan \beta, \mu_{\text{eff}} = \lambda \langle S \rangle, A_\lambda, \tilde{m}_S$ and $m_A^2 = \frac{2}{\sin 2\beta} (\mu A_\lambda + \lambda \xi_F M_n^2)$ as input parameters for the nMSSM[14].

The scalar fields H_u, H_d and S can be expanded as

$$H_d = \begin{pmatrix} \frac{v_d + \phi_d + i\varphi_d}{\sqrt{2}} \\ H_d^- \end{pmatrix}, \quad H_u = \begin{pmatrix} H_u^+ \\ \frac{v_u + \phi_u + i\varphi_u}{\sqrt{2}} \end{pmatrix}, \quad S = \frac{1}{\sqrt{2}} (s + \sigma + i\xi), \quad (9)$$

and the mass eigenstates are obtained by diagonalizing the Higgs mass matrices:

$$\begin{pmatrix} h_1 \\ h_2 \\ h_3 \end{pmatrix} = U^H \begin{pmatrix} \phi_u \\ \phi_d \\ \sigma \end{pmatrix}, \quad \begin{pmatrix} a \\ A \\ G^0 \end{pmatrix} = U^A \begin{pmatrix} \varphi_u \\ \varphi_d \\ \xi \end{pmatrix}, \quad \begin{pmatrix} H^+ \\ G^+ \end{pmatrix} = U \begin{pmatrix} H_u^+ \\ H_d^+ \end{pmatrix}, \quad (10)$$

where h_1, h_2, h_3 and a, A are respectively the CP-even and CP-odd neutral Higgs bosons, G^0 and G^+ are Goldstone bosons, and H^+ is the charged Higgs boson. So both the nMSSM and NMSSM predict three CP-even Higgs bosons, two CP-odd Higgs bosons and one pair of charged Higgs bosons. Note the lighter CP-odd Higgs a in these model is the mixture of the singlet field ξ and the doublet field $\cos \beta \varphi_u + \sin \beta \varphi_d$ with its couplings to down-type quarks and charged leptons proportional to $\frac{g}{m_W \cos \beta} U_{12}^A$. So for singlet dominated a , the couplings are suppressed by U_{12}^A . As a comparison, the interactions of a with the squarks are not suppressed by such a factor[7].

III. CALCULATIONS

In the Type-II 2HDM, L2HDM, nMSSM and NMSSM, the rare Z -decays $Z \rightarrow \bar{f} f a$ ($f = b, \tau$), $Z \rightarrow a a a$ and $Z \rightarrow a \gamma$ may proceed by the Feynman diagrams shown in Fig.1, Fig.2 and Fig.3 respectively. For these diagrams, the intermediate state h represents all possible CP-even Higgs bosons in the corresponding model, i.e. h_1 and h_2 in Type-II 2HDM

and L2HDM and h_1 , h_2 and h_3 in nMSSM and NMSSM. In order to take into account possible resonance effects of h in Fig.1(c) and Fig.2 (a), we have calculated all the decay modes of h and properly included the width effect in its propagator.

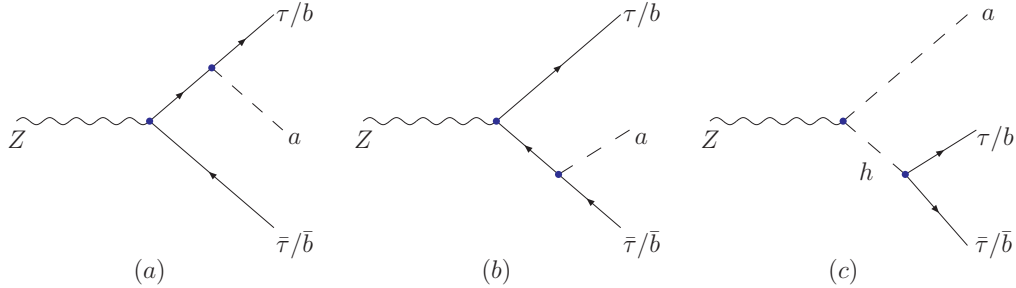


FIG. 1: Feynman diagrams contributing to the decay $Z \rightarrow \bar{f} f a$ ($f = b, \tau$) in new physics models. h denotes all possible intermediate CP-even Higgs bosons in the corresponding model.

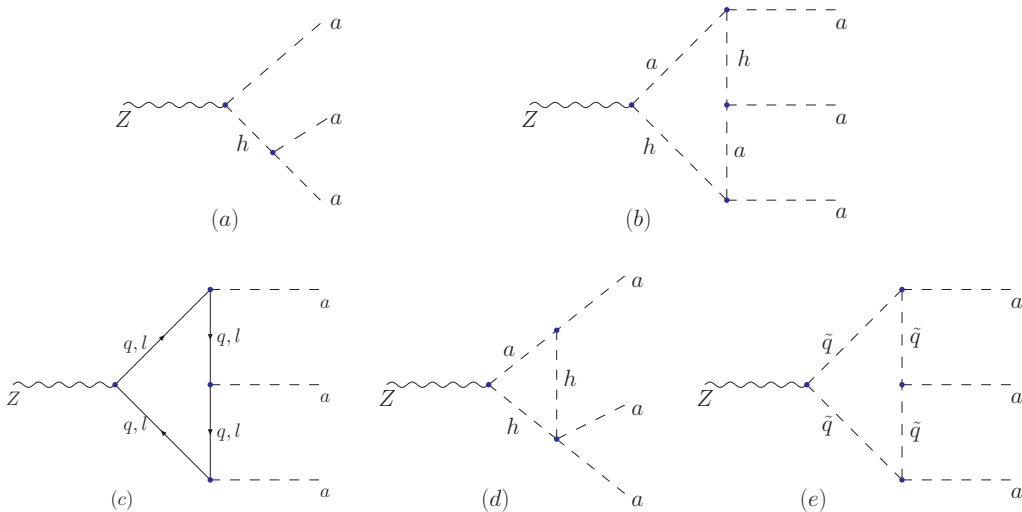


FIG. 2: Feynman diagrams contributing to the decay $Z \rightarrow a a a$ in new physics models. Note the last diagram only exists in the nMSSM and NMSSM.

As for the rare decay $Z \rightarrow a a a$, besides the tree level contribution shown in Fig.2 (a), loop diagrams may also be important for the case of large $h a a$ coupling. So we consider all these contributions in our calculation. Unlike the decay $Z \rightarrow \bar{f} f a$ and $Z \rightarrow a a a$, the decay $Z \rightarrow a \gamma$ occurs only at loop level, so in general its rate should be much smaller than the other two. In Appendix A and B, we list the lengthy amplitudes for the diagrams in Fig.2 (b-e) and in Fig.3 respectively.

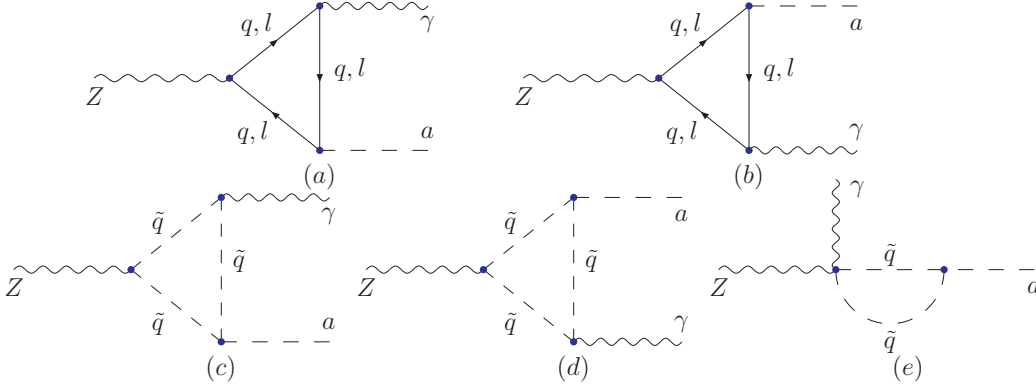


FIG. 3: Feynman diagrams contributing to the decay $Z \rightarrow a\gamma$ at one-loop level in new physics models. Note the last three diagrams (c-e) only exist in the nMSSM and NMSSM.

IV. NUMERICAL RESULTS AND DISCUSSIONS

For the Type-II 2HDM and L2HDM, we consider the following constraints [15]:

- (1) Theoretical constraints on λ_i from perturbativity, unitarity and requirements that the scalar potential is finite at large field values and contains no flat directions [18, 20].
- (2) The constraints from the LEP search for neutral Higgs bosons. We compute the signals from the Higgs-strahlung production $e^+e^- \rightarrow ZH_i$ ($H_i = h, H$) with $H_i \rightarrow 2b, 2\tau, 4b, 4\tau, 2b2\tau$ [21, 22] and from the associated production $e^+e^- \rightarrow H_i A$ with $H_i A \rightarrow 4b, 4\tau, 2b2\tau, 6b, 6\tau$ [23] and compare them with their LEP data. We also consider the constraints from $e^+e^- \rightarrow ZH_i$ by looking for a peak of M_{H_i} recoil mass distribution of Z -boson [24] and the constraint of $\Gamma(Z \rightarrow H_i A) < 5.8$ MeV when $m_A + m_{H_i} < m_Z$ [25].
- (3) The constraints from the LEP search for a light Higgs boson via the Yukawa process $e^+e^- \rightarrow \bar{f}fS$ with $f = b, \tau$ and S denoting a scalar [26]. These constraints can limit $\bar{f}fS$ coupling versus m_S in new physics models.
- (4) The constraints from $Z\tau^+\tau^-$ couplings. For a large $\tan\beta$ the Higgs sector can give sizable radiative corrections to $Z\tau^+\tau^-$ couplings. We calculate such corrections and require the corrected $Z\tau^+\tau^-$ couplings to lie within the 2σ range of their fitted value. The SM prediction for this coupling at Z -pole is given by $g_V^{SM} = -0.03712$ and $g_A^{SM} = -0.50127$ [27], and the fitted value given respectively by -0.0366 ± 0.00245

and -0.50204 ± 0.00064 [27]. We use the formula in [28] in our calculation.

- (5) The constraints from τ leptonic decay. We require the new physics correction to the branching ratio $Br(\tau \rightarrow e\bar{\nu}_e\nu_\tau)$ to be in the range of $-0.80\% \sim 1.21\%$ [29]. We use the formula in [29] in our calculation.
- (6) Indirect constraints from precision electroweak observables such as ρ_ℓ , $\sin^2\theta_{eff}^\ell$ and M_W , or their combinations $\epsilon_i(i = 1, 2, 3)$ [30]. We require ϵ_i to be compatible with the LEP/SLD data at 95% confidence level. Also, for $R_b = \Gamma(Z \rightarrow \bar{b}b)/\Gamma(Z \rightarrow \text{hadrons})$ whose measured value is $R_b^{exp} = 0.21629 \pm 0.00066$ and the SM prediction is $R_b^{SM} = 0.21578$ for $m_t = 173$ GeV [31], we require new physics prediction of R_b is within the 2σ range of its experimental value.
- (7) The constraints from B physics observables such as the branching ratios for $B \rightarrow X_s\gamma$, $B_s \rightarrow \mu^+\mu^-$ and $B^+ \rightarrow \tau^+\nu_\tau$, and the mass difference ΔM_d and ΔM_s . We require their theoretical predications to agree with the corresponding experimental values at 2σ level. For the Type-II 2HDM, this is equivalent to require $m_{H^+} > 316\text{GeV}$ [32]; while for the L2HDM, since the coupling of the charged Higgs boson to bottom quark is not enhanced by $\tan\beta$, there is no essentially constraint on m_{H^+} [33]. In our analysis, we impose the LEP bound on m_{H^+} , i.e. $m_{H^+} > 92\text{GeV}$ [34].
- (8) The constraint from $\Upsilon \rightarrow a\gamma$. We use the latest BaBar limits on $Br(\Upsilon(3S) \rightarrow a\gamma \rightarrow \tau^+\tau^-\gamma, \mu^+\mu^-\gamma)$ to constrain the $\bar{b}ba$ coupling in new physics models [12].
- (9) The constraints from the muon anomalous magnetic moment $a_\mu^{exp} - a_\mu^{SM} = (25.5 \pm 8.0) \times 10^{-10}$ [35]. We require the L2HDM to explain the difference at 2σ level[15], while for the Type-II 2HDM, we require it to explain a_μ at 3σ level since this model is difficult to enhance the a_μ significantly[36].
- (10) Since the CP-odd Higgs A can be quite light and $h, H \rightarrow AA$ may open up with a large decay width, we require the width of any Higgs boson in new physics model to be smaller than its mass (otherwise the Higgs boson may be too fat).

With the above constraints, we scan over the parameter space of the Type-II 2HDM and the L2HDM in the ranges:

$$\begin{aligned}
1 \leq \tan \beta \leq 80, \quad -\sqrt{2}/2 \leq \sin \alpha \leq \sqrt{2}/2, \quad m_a \leq 30 \text{ GeV}, \quad \lambda_5 \leq 4\pi, \\
5 \text{ GeV} \leq m_{h_1, h_2} \leq 500 \text{ GeV}, \quad 316 \text{ GeV}(92\text{GeV}) \leq m_{H^+} \leq 500 \text{ GeV}.
\end{aligned}
\tag{11}$$

For the nMSSM and NMSSM, in addition to the above constraints, we also consider the following constraints:

- (a) Direct bounds on sparticle masses from the LEP1, the LEP2 and the Tevatron experiments [31].
- (b) The LEP1 bound on invisible Z decay $\Gamma(Z \rightarrow \tilde{\chi}_1^0 \tilde{\chi}_1^0) < 1.76 \text{ MeV}$; the LEP2 bound on neutralino production $\sigma(e^+e^- \rightarrow \tilde{\chi}_1^0 \tilde{\chi}_i^0) < 10^{-2} \text{ pb}$ ($i > 1$) and $\sigma(e^+e^- \rightarrow \tilde{\chi}_i^0 \tilde{\chi}_j^0) < 10^{-1} \text{ pb}$ ($i, j > 1$)[37].
- (c) Dark matter constraints from the WMAP relic density $0.0975 < \Omega h^2 < 0.1213$ [38].

Note that, for the NMSSM, most of the above constraints have been encoded in NMSSM-Tools [39]. In our calculations we complement the code by adding the constraints (3-6). We also extend the code to the nMSSM. With the above constraints, we scrutinize the parameters of the NMSSM in the ranges:

$$\begin{aligned}
0.1 \leq \lambda, \kappa \leq 0.7, \quad 1 \leq \tan \beta \leq 80, \quad 100 \text{ GeV} \leq m_A \leq 1 \text{ TeV}, \\
50 \text{ GeV} \leq \mu_{\text{eff}}, M_1 \leq 500 \text{ GeV}, \quad -100 \text{ GeV} \leq A_\kappa \leq 100 \text{ GeV},
\end{aligned}
\tag{12}$$

and the parameters of the nMSSM in the following ranges[14]:

$$\begin{aligned}
0.1 \leq \lambda \leq 0.7, \quad 1 \leq \tan \beta \leq 80, \quad 100 \text{ GeV} \leq m_A \leq 1 \text{ TeV}, \\
50 \text{ GeV} \leq \mu_{\text{eff}}, M_1 \leq 500 \text{ GeV}, \quad -1 \text{ TeV} \leq A_\lambda \leq 1 \text{ TeV}, \quad 0 \leq \tilde{m}_S \leq 200\text{GeV}.
\end{aligned}
\tag{13}$$

In order to reduce the number of relevant soft parameters, we adopt the so-called m_h^{max} scenario, which assumes that the soft mass parameters for the third generation squarks are degenerate: $M_{Q_3} = M_{U_3} = M_{D_3} = 800 \text{ GeV}$, and that the trilinear couplings of the third generation squarks are also degenerate, $A_t = A_b$ with $X_t = A_t - \mu \cot \beta = -2M_{Q_3}$. Moreover, for the slepton sector we assume all the soft-breaking masses and trilinear parameters to be 100 GeV. This setting is necessary for the nMSSM since this model is difficult to explain the

muon anomalous moment at 2σ level for heavy sleptons[14]. Finally, we assume the grand unification relation $3M_1/5\alpha_1 = M_2/\alpha_2 = M_3/\alpha_3$ for the gaugino masses with α_i being fine structure constants of the different gauge group.

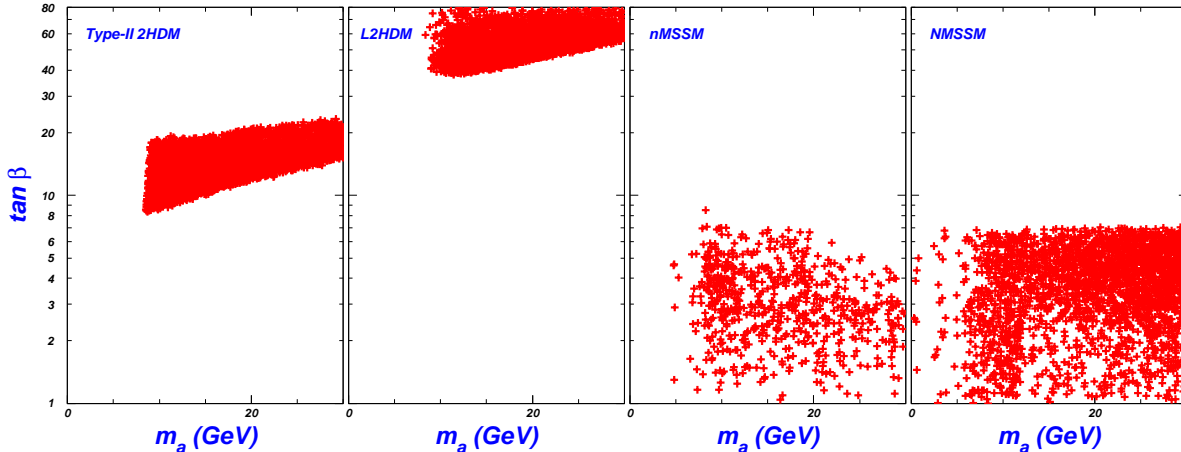


FIG. 4: The scattering plot of the surviving samples projected on $m_a - \tan \beta$ plane.

With large number of random points in the scans, we finally get about 3000, 4000, 800 and 2000 samples for the Type-II 2HDM, the L2HDM, the nMSSM and the NMSSM respectively which satisfy $m_a \leq 30\text{GeV}$. Analyzing the properties of the a indicates that in the nMSSM and the NMSSM, its dominant component is the singlet field so that its couplings with the SM fermions are suppressed[10, 14]. Our analysis also indicates that the main decay products of a are $\bar{\tau}\tau$ for the L2HDM[15], $\bar{b}b$ (dominant) and $\bar{\tau}\tau$ (subdominant) for the Type-II 2HDM, the nMSSM and the NMSSM, and in some rare cases, neutralino pairs in the nMSSM[14]. In Fig.4, we project the surviving samples on the $m_a - \tan \beta$ plane. This figure shows that the allowed range of $\tan \beta$ is from 8 to 20 in the Type-II 2HDM, and from 37 to 80 in the L2HDM. These results can be understood as follows: the lower bounds of $\tan \beta$ come from the fact that we require the models to explain the muon anomalous moment, while the upper bound is due to we have imposed the constraint from the LEP process $e^+e^- \rightarrow \bar{b}bS \rightarrow 4b$, which have limited the upper reach of the $\bar{b}bS$ coupling for light S [26](for the dependence of $\bar{b}bS$ coupling on $\tan \beta$, see Sec. II). This figure also indicates that for the nMSSM and the NMSSM, $\tan \beta$ is upper bounded by 10. For the nMSSM, this is because large $\tan \beta$ can suppress the dark matter mass to make its annihilation difficult[14], but for the NMSSM, this is because we choose a light slepton mass so that large $\tan \beta$ can enhance a_μ too significantly to be acceptable by relevant experiments. We checked that for

the slepton mass as heavy as 300GeV, $\tan\beta \geq 25$ is still allowed for the NMSSM.

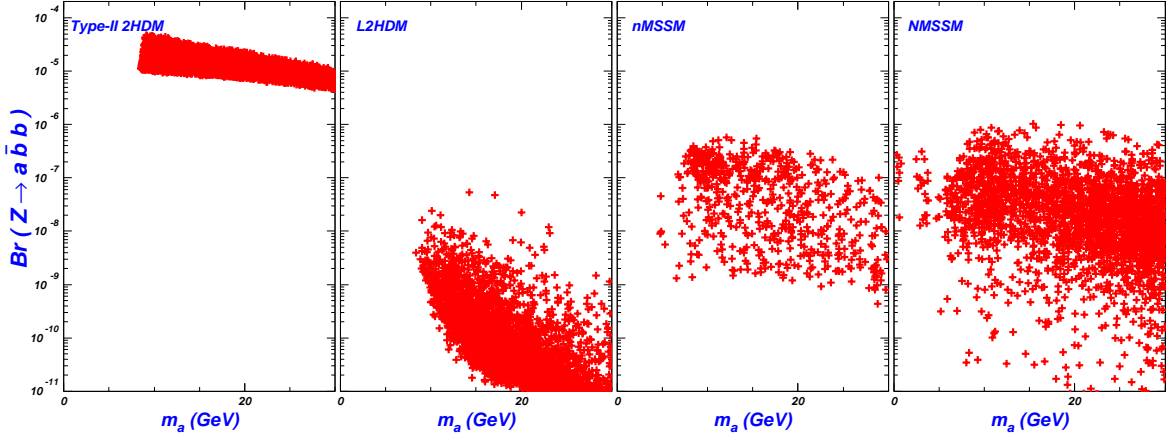


FIG. 5: Same as Fig.4, but for the branching ratio of $Z \rightarrow \bar{b}ba$ versus m_a .

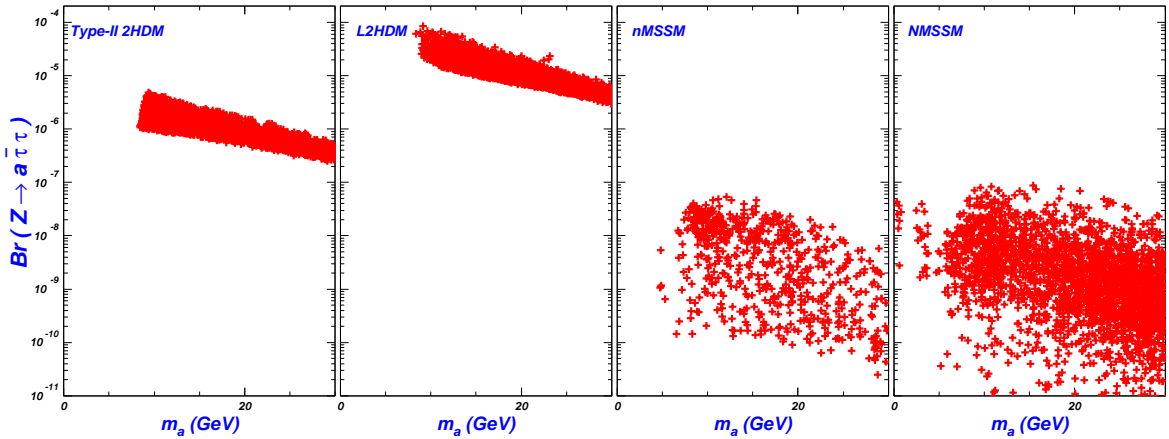


FIG. 6: Same as Fig.5, but for $Z \rightarrow \bar{\tau}\tau a$.

In Fig.5 and Fig.6, we show the branching ratios of $Z \rightarrow \bar{b}ba$ and $Z \rightarrow \bar{\tau}\tau a$ respectively. Fig.5 indicates, among the four models, the Type-II 2HDM predicts the largest ratio for $Z \rightarrow \bar{b}ba$ with its value varying from 4×10^{-6} to 6×10^{-5} . The underlying reason is in the Type-II 2HDM, the $\bar{b}ba$ coupling is enhanced by $\tan\beta$ (see Fig.4), while in the other three model, the coupling is either not enhanced or suppressed by the singlet component of the a . Fig.6 shows that the L2HDM predicts the largest rate for $Z \rightarrow \bar{\tau}\tau a$ with its value reaching 10^{-4} in optimum case, and for the other three models, the ratio of $Z \rightarrow \bar{\tau}\tau a$ is about one order smaller than that of $Z \rightarrow \bar{b}ba$. This feature can be easily understood from the $\bar{\tau}\tau a$ coupling introduced in Sect. II. Here we emphasize that, if the nature prefers the existence of a light a , $Z \rightarrow \bar{b}ba$ and/or $Z \rightarrow \bar{\tau}\tau a$ in the Type-II 2HDM and the L2HDM will be

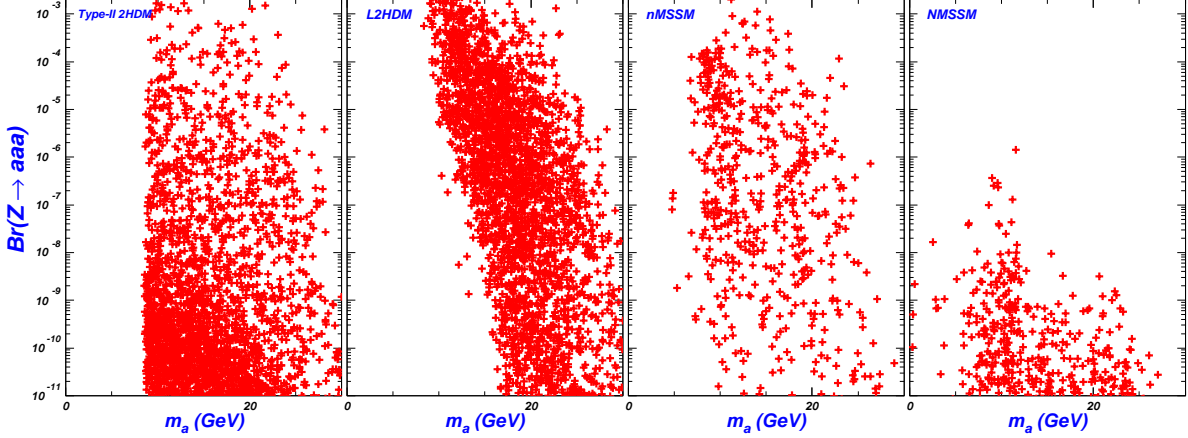


FIG. 7: Same as Fig.5, but for $Z \rightarrow aaa$.

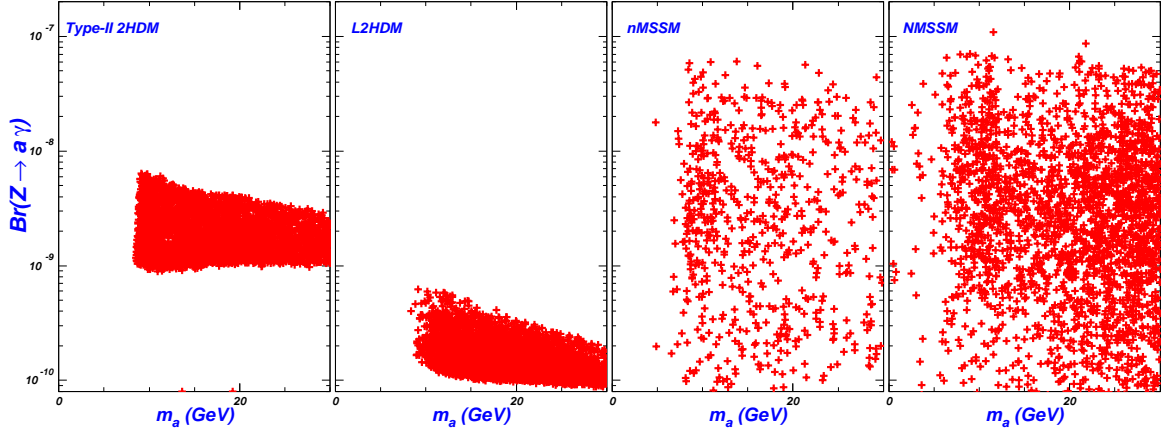


FIG. 8: Same as Fig.5, but for $Z \rightarrow a\gamma$.

observable at the GigaZ. Then by the rates of the two decays, one can determine whether the Type-II 2HDM or the L2HDM is the right theory. On the other hand, if both decays are observed with small rates or fail to be observed, the singlet extensions of the MSSM are favored.

Fig.5 and Fig.6 shows that the rates of $Z \rightarrow \bar{b}ba$ and $Z \rightarrow \bar{\tau}\tau a$ in the nMSSM and the NMSSM are quite similar for moderate $\tan\beta$, so in order to distinguish the two models, we consider another decay mode $Z \rightarrow aaa$. The branching ratio of this decay is plotted in Fig.7 where one can learn that the $Br(Z \rightarrow aaa)$ can be larger than any of $Z \rightarrow \bar{f}fa$ ($f = b, \tau$) decay, reaching 10^{-3} in the optimum cases of the Type-II 2HDM, the L2HDM and the nMSSM. A detailed study shows that the dominant contributions are from the tree-level diagram Fig.3 (a) and the Higgs-induced loop diagram Fig.3(b) due to the possible large couplings g_{haa} . Our study also indicates that, in some cases, the intermediate state h in

Fig.3 (a) may be on-shell. In fact, we found this is the main difference between the nMSSM and the NMSSM, i.e. in the nMSSM, h in Fig.3 (a) may be on-shell while in the NMSSM, it never does, and that is why the size of the decay in the models may differ greatly. So we conclude that the decay $Z \rightarrow aaa$ may serve as an alternative channel to test new physics model, especially it can be used to distinguish the nMSSM and the NMSSM.

Finally we show the rate of $Z \rightarrow a\gamma$ as the function of m_a in Fig.8. This decay proceeds only by loops mediated by quarks/leptons in the Type-II 2HDM and L2HDM, and has additional contribution from loops mediated by squarks in the supersymmetric models (see Fig.3). Fig.8 then indicates that its branching ratio is of the order of 10^{-9} in the Type-II 2HDM and 10^{-10} in the L2HDM, too small to be detectable at the GigaZ. In contrast, the rate can reach 10^{-8} in the nMSSM and NMSSM which may be accessible at the GigaZ. So we conclude that the decay $Z \rightarrow a\gamma$ may also provide useful information to differentiate the new physics models.

V. CONCLUSION

In this paper, we studied the rare Z -decays $Z \rightarrow \bar{f}fa$ ($f = b, \tau$), $Z \rightarrow aaa$ and $Z \rightarrow a\gamma$ in the Type-II 2HDM, lepton-specific 2HDM, nMSSM and NMSSM, which predict a light CP-odd Higgs boson a . In the parameter space allowed by current experiments, the branching ratio can be as large as 10^{-4} for $Z \rightarrow \bar{f}fa$, 10^{-3} for $Z \rightarrow aaa$ and 10^{-8} for $Z \rightarrow a\gamma$, which should be accessible at the GigaZ option. Since different models predict different size of branching ratios, they could be distinguished at the GigaZ through the measurement of these rare decays.

Acknowledgment

This work was supported in part by HASTIT under grant No. 2009HASTIT004, by the National Natural Science Foundation of China (NNSFC) under grant Nos. 10821504, 10725526 and 10635030, and by the Project of Knowledge Innovation Program (PKIP) of Chinese Academy of Sciences under grant No. KJCX2.YW.W10.

Appendix A: Amplitude of $Z \rightarrow aaa$

Here we list the loop level amplitudes of the process $Z(p_z, \epsilon) \rightarrow a(p_1)a(p_2)a(p_3)$. Their expressions are given by

$$\mathcal{M}^b = \frac{1}{16\pi^2} \sum_{h_i, h_j} g_{zh_i a} g_{h_i a a} g_{h_j a a} g_{h_j a a} (2D_\mu^1 - p_{z\mu} D_0^1) \epsilon^\mu(p_z) \quad (\text{A1})$$

$$\begin{aligned} \mathcal{M}^c = & \frac{1}{16\pi^2} 2m_q g_{zqq} g_{aqq} \{ [(p_2 \cdot p_3) p_{1\mu} - (p_1 \cdot p_3) p_{2\mu} + (p_1 \cdot p_2) p_{3\mu}] D_0^2 \\ & + C_0^{21} p_{1\mu} + C_0^{22} p_{3\mu} \} \epsilon^\mu(p_z) \end{aligned} \quad (\text{A2})$$

$$\mathcal{M}^d = -\frac{1}{16\pi^2} g_{zh_i a} g_{h_j a a} g_{h_i h_j a a} (2C_\mu^3 - p_{z\mu} C_0^3) \epsilon^\mu(p_z) \quad (\text{A3})$$

$$\mathcal{M}^e = -\frac{1}{16\pi^2} g_{a\tilde{q}_i \tilde{q}_j} g_{a\tilde{q}_j \tilde{q}_k} g_{a\tilde{q}_k \tilde{q}_l} g_{z\tilde{q}_i \tilde{q}_l} (2D_\mu^4 - p_{z\mu} D_0^4) \epsilon^\mu(p_z) \quad (\text{A4})$$

where g_{zqq} and g_{aqq} are the coupling coefficient of quark/lepton to Z boson and CP-odd Higgs boson, respectively; $g_{h_i h_j a a}$ is the coupling of two CP-even Higgs and two CP-odd Higgs bosons; $g_{z\tilde{q}\tilde{q}}$ and $g_{a\tilde{q}\tilde{q}}$ are the couplings of squark to Z-boson and CP-odd Higgs boson, respectively.

For the above loop functions, we adopt the definition in [40] and use the LoopTools [41] in our calculations. The loop functions' dependence is given by

$$D^1 = D(-p_1, -p_2, -p_3, m_a^2, m_{h_j}^2, m_a^2, m_{h_i}^2) \quad (\text{A5})$$

$$C^{21} = C(-p_1, p_1 - p_z, m_q^2, m_q^2, m_q^2) \quad (\text{A6})$$

$$C^{22} = C(-p_z, p_3, m_q^2, m_q^2, m_q^2) \quad (\text{A7})$$

$$D^2 = D(-p_1, -p_2, -p_3, m_q^2, m_q^2, m_q^2, m_q^2) \quad (\text{A8})$$

$$C^3 = C(-p_1, p_1 - p_z, m_a^2, m_{h_j}^2, m_{h_i}^2) \quad (\text{A9})$$

$$D^4 = D(-p_1, -p_2, -p_3, m_{\tilde{q}_i}^2, m_{\tilde{q}_j}^2, m_{\tilde{q}_k}^2, m_{\tilde{q}_l}^2) \quad (\text{A10})$$

where m_a , m_{h_i} and $m_{\tilde{q}_i}$ are the mass of CP-odd Higgs, CP-even Higgs and squark, respectively.

Appendix B: Amplitude of $Z \rightarrow a\gamma$

Here we give the amplitudes of process $Z(p_z, \epsilon_1) \rightarrow a(p_1)\gamma(p_2, \epsilon_2)$. Their expressions are given by

$$\mathcal{M}^a = \frac{1}{16\pi^2} A_1 g_{aqq} \{ -4im_q A_2 \epsilon_{\mu\rho\lambda\nu} p_z^\rho p_2^\lambda C_0^1 + 2m_q [2(p_2 - p_z)_\mu C_\nu^1 + (p_{z\mu} p_{2\nu} - p_{2\mu} p_{z\nu}) C_0^1 + g_{\mu\nu} B_0^1 - 2g_{\mu\nu} p_2^\lambda C_\lambda^1 + g_{\mu\nu} (p_z \cdot p_2) C_0^1] \} \epsilon_1^\mu(p_z) \epsilon_2^\nu(p_2) \quad (\text{B1})$$

$$\mathcal{M}^b = \frac{1}{16\pi^2} A_1 g_{aqq} \{ -4im_q A_2 \epsilon_{\mu\rho\lambda\nu} p_z^\rho p_1^\lambda C_0^1 + 2m_q [-2p_{1\mu} C_\nu^2 + (p_{z\mu} p_{1\nu} + p_{1\mu} p_{z\nu}) C_0^2 - g_{\mu\nu} B_0^2 + 2g_{\mu\nu} p_1^\lambda C_\lambda^2 - g_{\mu\nu} (p_z \cdot p_1) C_0^2] \} \epsilon_1^\mu(p_z) \epsilon_2^\nu(p_2) \quad (\text{B2})$$

$$\mathcal{M}^c = \frac{1}{16\pi^2} A_3 g_{z\tilde{q}_i\tilde{q}_k} g_{a\tilde{q}_j\tilde{q}_k} \delta^{ij} (4C_{\mu\nu}^3 - 2p_{2\nu} C_\mu^3 - 2p_{z\mu} C_\nu^3 + p_{z\mu} p_{2\nu} C_0^3) \epsilon_1^\mu(p_z) \epsilon_2^\nu(p_2) \quad (\text{B3})$$

$$\mathcal{M}^d = \frac{1}{16\pi^2} A_3 g_{z\tilde{q}_i\tilde{q}_k} g_{a\tilde{q}_j\tilde{q}_k} \delta^{ij} (4C_{\mu\nu}^4 - 2(p_1 + p_z)_\nu C_\mu^4 - 2p_{z\mu} C_\nu^4 + p_{z\mu} (p_1 + p_z)_\nu C_0^4) \epsilon_1^\mu(p_z) \epsilon_2^\nu(p_2) \quad (\text{B4})$$

$$\mathcal{M}^e = -\frac{1}{16\pi^2} 2A_3 g_{z\tilde{q}_i\tilde{q}_j} g_{a\tilde{q}_i\tilde{q}_j} B_0^5 \epsilon_1^\mu(p_z) \epsilon_2^\nu(p_2) \quad (\text{B5})$$

with $A_1 = \frac{e^2}{3 \sin \theta_W \cos \theta_W}$, $A_2 = \frac{1}{2} - \frac{4}{3} \sin^2 \theta_W$ for top quark induced loop diagram; $A_1 = \frac{e^2}{6 \sin \theta_W \cos \theta_W}$, $A_2 = \frac{1}{2} - \frac{2}{3} \sin^2 \theta_W$ for bottom quark induced loop diagram; $A_1 = \frac{e^2}{2 \sin \theta_W \cos \theta_W}$, $A_2 = \frac{1}{2} - 2 \sin^2 \theta_W$ for tau induced loop diagram; $A_3 = \frac{2\epsilon}{3}$ for top squark induced loop diagram; $A_3 = -\frac{\epsilon}{3}$ for bottom squark induced loop diagram.

The loop functions' dependence is given by

$$C^1 = C(-p_2, -p_1, m_q^2, m_q^2, m_q^2) \quad (\text{B6})$$

$$B^1 = B(-p_1, m_q^2, m_q^2) \quad (\text{B7})$$

$$C^2 = C(-p_1, -p_2, m_q^2, m_q^2, m_q^2) \quad (\text{B8})$$

$$B^2 = B(-p_2, m_q^2, m_q^2) \quad (\text{B9})$$

$$C^3 = C(-p_2, -p_1, m_{\tilde{q}_i}^2, m_{\tilde{q}_j}^2, m_{\tilde{q}_k}^2) \quad (\text{B10})$$

$$C^4 = C(-p_1, -p_2, m_{\tilde{q}_i}^2, m_{\tilde{q}_j}^2, m_{\tilde{q}_k}^2) \quad (\text{B11})$$

$$B^5 = B(-p_1, m_{\tilde{q}_i}^2, m_{\tilde{q}_j}^2) \quad (\text{B12})$$

[1] J. A. Aguilar-Saavedra *et al.*, hep-ph/0106315.

[2] For some reviews, see, e.g., M. A. Perez, G. Tavares-Velasco and J. J. Toscano, Int. J. Mod. Phys. A **19**, 159 (2004); J. M. Yang, arXiv:1006.2594.

- [3] See, e.g., M. Frank and H. Hamidian, Phys. Rev. D **54**, 6790 (1996); J. I. Illana, T. Riemann, Phys. Rev. D **63**, 053004 (2001); J. I. Illana, M. Masip, Phys. Rev. D **67**, 035004 (2003); M. A. Mughal, M. Sadiq, K. Ahmed, Phys. Lett. B **417**, 87 (1998); J. Cao, Z. Xiong, J. M. Yang, Eur. Phys. J. C **32**, 245 (2004); J. Cao, L. Wu, J. M. Yang, Nucl. Phys. B **829**, 370 (2010); D. Delepine and F. Vissani, Phys. Lett. B **522**, 95 (2001); M. A. Perez and M. A. Soriano, Phys. Rev. D **46**, 284 (1992); M. Frank, Phys. Rev. D **62**, 053004 (2000); Phys. Rev. D **65**, 033011 (2002); A. Ghosal, Y. Koide, and H. Fusaoka, Phys. Rev. D **64**, 053012 (2001); P. Langaker and M. Plumacher, Phys. Rev. D **62**, 013006 (2000); C. Yue, H. Li, Y. M. Zhang, and Y. Jia, Phys. Lett. B **536**, 67 (2002); E. O. Iltan and I. Turan, Phys. Rev. D **65**, 013001 (2002); J. Bernabeu *et al.*, Phys. Lett. B **187**, 303 (1987); Phys. Lett. B **197**, 418 (1987); G. Eilam and T. Rizzo, Phys. Lett. B **188**, 91 (1987); G. Korner *et al.*, Phys. Lett. B **300**, 381 (1993); A. Ilakovac and A. Pilaftis, Nucl. Phys. B **437**, 491 (1995); T. K. Kuo and N. Nakagawa, Phys. Rev. D **32**, 306 (1985); M. J. S. Levine, Phys. Rev. D **36**, 1329 (1987); M. A. Doncheski *et al.*, Phys. Rev. D **40**, 2301 (1989); Bhattacharyya *et al.*, Phys. Rev. D **42**, 268 (1990); E. Nardi, Phys. Rev. D **48**, 1240 (1993); A. Mendez and L. M. Mir, Phys. Rev. D **40**, 251 (1989); Z. K. Silagadze, Phys. Scripta **64**, 128 (2001).
- [4] A. Axelrod, Nucl. Phys. B **209**, 349 (1982); M. Clements *et al.*, Phys. Rev. D **27**, 570 (1983); V. Ganapathi, Phys. Rev. D **27**, 579 (1983); W. S. Hou *et al.*, Phys. Rev. Lett. **57**, 1406 (1986); J. Bernabeu *et al.*, Phys. Rev. Lett. **57**, 1514 (1986); C. Bush, Nucl. Phys. B **319**, 15 (1989); W. S. Hou and R. G. Stuart, Phys. Lett. B **226**, 122 (1989); B. Grzadkowski *et al.*, Phys. Lett. B **268**, 106 (1991); D. Atwood, L. Reina, and A. Soni, Phys. Rev. D **55**, 3156 (1997); B. Mukhopadhyaya and A. Raychaudhuri, Phys. Rev. D **39**, 280 (1989); M. J. Duncan, Phys. Rev. D **31**, 1139 (1985); F. Gabbiani *et al.*, Phys. Lett. B **214**, 398 (1988); M. Chemtob and G. Moreau, Phys. Rev. D **59**, 116012 (1999); D. Atwood *et al.*, Phys. Rev. D **66**, 093005 (2002); G. T. Park, and T. K. Kuo, Phys. Rev. D **42**, 3879 (1990); X. Zhang and B. L. Young, Phys. Rev. D **51**, 6584 (1995); W. Buchmuller and M. Gronau, Phys. Lett. B **220**, 641 (1989); J. Roldan, F. J. Botella, and J. Vidal, Phys. Lett. B **283**, 389 (1992); X. L. Wang, G. R. Lu, and Z. J. Xiao, Phys. Rev. D **51**, 4992 (1995).
- [5] D. Chang and W. Y. Keung, Phys. Rev. Lett. **77**, 3732 (1996); E. Keith and E. Ma, Phys. Rev. D **57**, 2017 (1998).
- [6] F. Larios, G. Tavares-Velasco and C. P. Yuan, Phys. Rev. D **64**, 055004 (2001); Phys. Rev. D

- 66**, 075006 (2002).
- [7] F. Franke and H. Fraas, *Int. J. Mod. Phys. A* **12** (1997) 479.
- [8] See, e.g., J. R. Ellis, J. F. Gunion, H. E. Haber, L. Roszkowski and F. Zwirner, *Phys. Rev. D* **39** (1989) 844; M. Drees, *Int. J. Mod. Phys. A* **4** (1989) 3635; U. Ellwanger, M. Rausch de Traubenberg and C. A. Savoy, *Phys. Lett. B* **315** (1993) 331; *Nucl. Phys. B* **492** (1997) 21; D.J. Miller, R. Nevzorov, P.M. Zerwas, *Nucl. Phys. B* **681**, 3 (2004).
- [9] P. Fayet, *Nucl. Phys. B* **90**, 104 (1975); C. Panagiotakopoulos, K. Tamvakis, *Phys. Lett. B* **446**, 224 (1999); *Phys. Lett. B* **469**, 145 (1999); C. Panagiotakopoulos, A. Pilaftsis, *Phys. Rev. D* **63**, 055003 (2001); A. Dedes, *et al.*, *Phys. Rev. D* **63**, 055009 (2001); A. Menon, *et al.*, *Phys. Rev. D* **70**, 035005 (2004); V. Barger, *et al.*, *Phys. Lett. B* **630**, 85 (2005). C. Balazs, *et al.*, *JHEP* **0706**, 066 (2007).
- [10] B. A. Dobrescu, K. T. Matchev, *JHEP* **0009**, 031 (2000); A. Arhrib, K. Cheung, T. J. Hou, K. W. Song, hep-ph/0611211; *JHEP* **0703**, 073 (2007); X. G. He, J. Tandean, and G. Valencia, *Phys. Rev. Lett.* **98**, 081802 (2007); *JHEP* **0806**, 002 (2008); F. Domingo *et al.*, *JHEP* **0901**, 061 (2009); Gudrun Hiller, *Phys. Rev. D* **70**, 034018 (2004); R. Dermisek, and John F. Gunion, *Phys. Rev. D* **75**, 075019 (2007); *Phys. Rev. D* **79**, 055014 (2009); *Phys. Rev. D* **81**, 055001 (2010); R. Dermisek, John F. Gunion, and B. McElrath, *Phys. Rev. D* **76**, 051105 (2007); Z. Heng, *et al.*, *Phys. Rev. D* **77**, 095012 (2008); A. Belyaev *et al.*, *Phys. Rev. D* **81**, 075021 (2010); D. Das and U. Ellwanger, arXiv:1007.1151 [hep-ph].
- [11] S. Andreas, O. Lebedev, S. Ramos-Sanchez and A. Ringwald, arXiv:1005.3978 [hep-ph].
- [12] J. F. Gunion, *JHEP* **0908**, 032 (2009); R. Dermisek and J. F. Gunion, *Phys. Rev. D* **81**, 075003 (2010).
- [13] R. Dermisek and J. F. Gunion, *Phys. Rev. Lett.* **95**, 041801 (2005); *Phys. Rev. D* **73**, 111701 (2006).
- [14] J. Cao, H. E. Logan, J. M. Yang, *Phys. Rev. D* **79**, 091701 (2009).
- [15] J. Cao, P. Wan, L. Wu, J. M. Yang, *Phys. Rev. D* **80**, 071701 (2009).
- [16] R. M. Barnett, *et al.*, *Phys. Lett. B* **136**, 191 (1984); R. M. Barnett, G. Senjanovic and D. Wyler, *Phys. Rev. D* **30**, 1529 (1984); Y. Grossman, *Nucl. Phys. B* **426**, 355 (1994).
- [17] H. S. Goh, L. J. Hall and P. Kumar, *JHEP* **0905**, 097 (2009); A. G. Akeroyd and W. J. Stirling, *Nucl. Phys. B* **447**, 3 (1995); A. G. Akeroyd, *Phys. Lett. B* **377**, 95 (1996); H. E. Logan and D. MacLennan, *Phys. Rev. D* **79**, 115022 (2009); M. Aoki, *et al.*, arXiv:0902.4665 [hep-ph].

- [18] J. F. Gunion and H. E. Haber, Phys. Rev. D **67**, 075019 (2003).
- [19] V. Barger, P. Langacker, H. S. Lee and G. Shaughnessy, Phys. Rev. D **73**, 115010 (2006).
- [20] A. G. Akeroyd, A. Arhrib and E. M. Naimi, Phys. Lett. B **490**, 119 (2000).
- [21] R. Barate *et al.*, Phys. Lett. B **565** (2003) 61.
- [22] OPAL collaboration, Eur. Phys. J. C **27** (2003) 483.
- [23] DELPHI Collaboration, Eur. Phys. J. C **38** (2004) 1.
- [24] D. Buskulic, *et al.*, Phys. Lett. B **313** (1993) 312; G. Abbiendi, *et al.*, Eur. Phys. J. C **27** (2003) 311.
- [25] K. Mönig, DELPHI 97-174 PHYS 748.
- [26] J.B. de Vivie and P. Janot [ALEPH Collaboration], PA13-027 contribution to the International Conference on High Energy Physics, Warsaw, Poland, 25–31 July 1996; J. Kurowska, O. Grajek and P. Zalewski [DELPHI Collaboration], CERN-OPEN-99-385.
- [27] [ALEPH Collaboration and DELPHI Collaboration and L3 Collaboration], Phys. Rept. **427**, 257 (2006).
- [28] J. Cao and J. M. Yang, JHEP **0812**, 006 (2008).
- [29] M. Krawczyk and D. Temes, Eur. Phys. J. C **44**, 435 (2005).
- [30] G. Altarelli and R. Barbieri, Phys. Lett. B **253**, 161 (1991); M. E. Peskin, T. Takeuchi, Phys. Rev. D **46**, 381 (1992).
- [31] C. Amsler, *et al.*, (Particle Data Group), Phys. Lett. B **667**, 1 (2008).
- [32] O. Deschamps, S. Descotes-Genon, S. Monteil, V. Niess, S. T’Jampens and V. Tisserand, arXiv:0907.5135 [hep-ph].
- [33] S. Su and B. Thomas, Phys. Rev. D **79**, 095014 (2009).
- [34] G. Abbiendi, *et al.*, Eur. Phys. J. C **32**, 453 (2004).
- [35] M. Davier, *et al.*, Eur. Phys. J. C **66**, 1 (2010).
- [36] K. Cheung, *et al.*, Phys. Rev. D **64**, 111301 (2001); K. Cheung and O. C. W. Kong, Phys. Rev. D **68**, 053003 (2003).
- [37] J. Abdallah *et al.*, Eur. Phys. J. C **31**, 421 (2004); G. Abbiendi *et al.*, Eur. Phys. J. C **35**, 1 (2004).
- [38] J. Dunkley *et al.* [WMAP Collaboration], Astrophys. J. Suppl. **180**, 306 (2009) [arXiv:0803.0586 [astro-ph]].
- [39] U. Ellwanger *et al.*, JHEP **02**, 066 (2005).

- [40] B. A. Kniehl, Phys. Rept. 240, 211 (1994).
- [41] T. Hahn, M. Perez-Victoria, Comput. Phys. Commun. **118**, 153 (1999); T. Hahn, Nucl. Phys. Proc. Suppl. **135**, 333 (2004).